



Camera Gap Removal in SOLIS/VSM Images

Andrew R. Marble, Lorraine Callahan & Alexei A. Pevtsov

National Solar Observatory

October 14, 2013

Abstract

The Vector Spectromagnetograph (VSM) instrument on the Synoptic Optical Long-term Investigations of the Sun (SOLIS) telescope is capable of obtaining spectropolarimetry for the full Sun (or a select latitudinal range) with $1''$ spatial resolution and 0.05\AA spectral resolution. This is achieved by scanning the Sun in declination and building up spectral cubes for multiple polarization states, utilizing a beamsplitter and two separate $2k \times 2k$ CCD cameras. As a result, the eastern and western hemispheres of the Sun are separated in preliminary VSM images by a vertical gap with soft edges and variable position and width. Prior to the comprehensive analysis presented in this document, a trial-and-error approach to removing the gap had yielded an algorithm that was inconsistent, undocumented, and responsible for incorrectly eliminating too many image columns. Here we describe, in detail, the basis for a new, streamlined, and properly calibrated prescription for locating and removing the gap that is correct to within approximately $1''$ (one column).

1 The Origin of the Gap

Initial images made with the Vector Spectromagnetograph (VSM) instrument on the Synoptic Optical Long-term Investigations of the Sun (SOLIS) telescope include a gap between the eastern and western hemispheres of the Sun (see Figure 1a). This gap corresponds to a physical separation in the focal plane of two halves of the solar disk image, where the width is determined by the positions of the cameras and optical train elements beyond the beamsplitter. As illustrated in Figure 1b, the (already dispersed) beam is spatially split into halves that are imaged onto two CCD cameras. To ensure no image loss, the cameras are illuminated such that there is a buffer on the order of tens of pixels between the spatially split edge of the beams and the corresponding end of the cameras. Thus, a gap devoid of illumination is present in the center of each row (Figure 2a) constructed by juxtaposing the camera images for each scan-line during Level 0-1 processing.

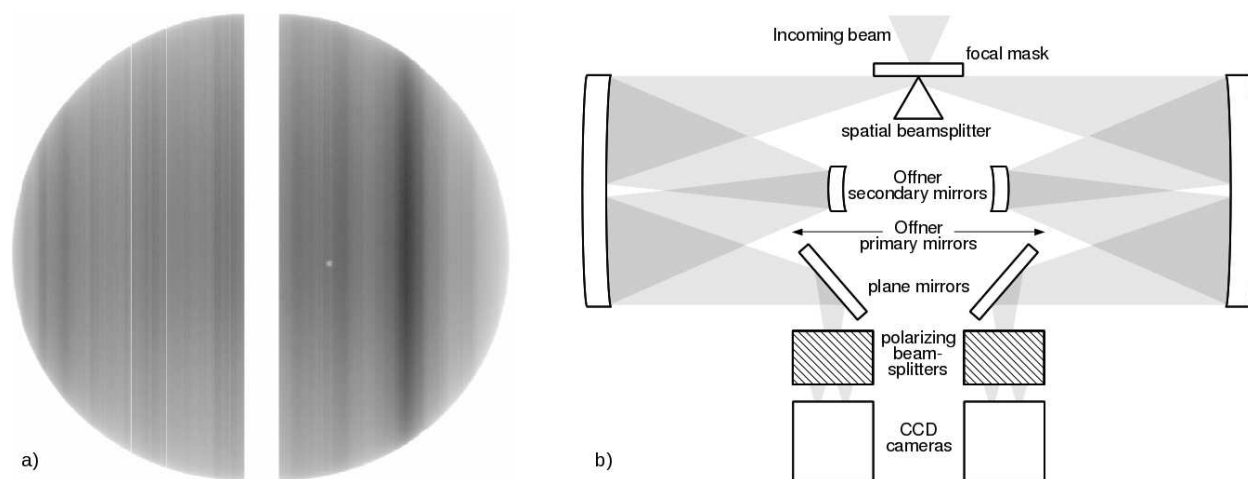


Figure 1 – (a) Level-1 6302L intensity image (without flat-field corrections) exhibiting the gap. (b) Schematic of the reimaging system within the VSM on SOLIS.

2 Relative Changes in the Gap Position/Size

Cursory inspection of the gap profile seen in flats shows that the position and width of the gap are not constant, but rather change both from day-to-day and throughout the day (due to various effects that likely include flexure and thermal expansion in the optical train beyond the beamsplitter; see Figure 1b). As an example, these two properties of the gap were measured (using a fiducial definition of the gap as where the normalized intensity falls below 50%) and plotted in Figure 2 for a day with an unusually large number of flats. Not only is the position of the gap shown to shift by four pixels throughout that particular day, but the width varied by more than twice as much during the afternoon hours (approximately three pixels an hour).

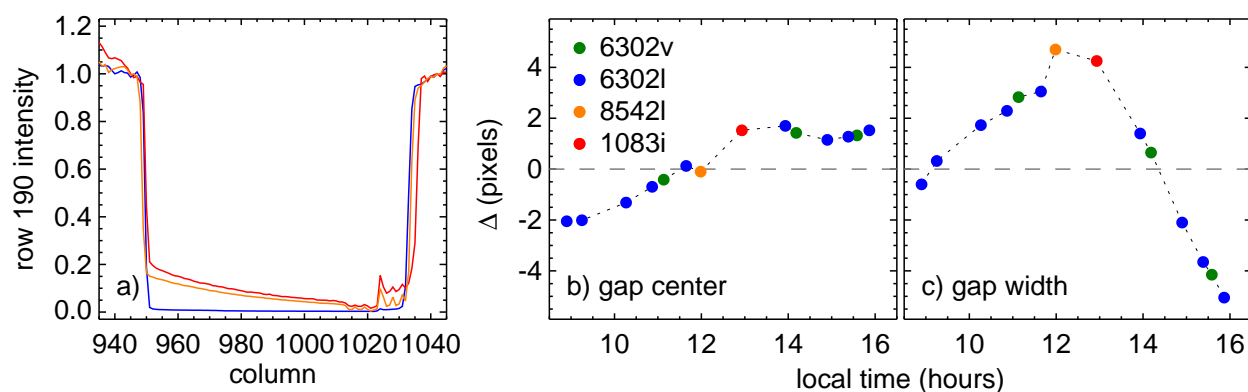


Figure 2 – Examples of the gap profile (a) from three flats taken on February 23, 2011 (separately normalized on both the left and right sides of the gap) and changes in the gap center (b) and width (c) from additional flats taken throughout the same day.

Thus, removal of the gap must be tailored for each observation in order to properly preserve the full solar disk as well as the spatial relationship between the halves to the left and right of the gap. The relatively rapid changes with time mean that identification of the gap should be based on an observation directly rather than its corresponding flat (as was done in the past; see Appendix A). More than 50% of the observations prior to September 2011 were paired with a flat taken at least 30 minutes before the mid-point of the observation, while 10% were separated in time by at least an hour.

Using the *central* row of the intensity image to characterize the gap further mitigates the significant time elapsed between the start and end of an observation. Based on Figure 2, the gap center/width shouldn't change by more than a half/whole pixel during the 20 minute interval between observing the disk center and either pole for 8542L (the longest observation). There have been undocumented references to gaps with tilts somewhat larger than this; however, casual inspection of the gap profile can be misleading due to lack of reliable flat-fielding within the gap (where the cameras are not illuminated well or at all) and careful analysis is hindered by the fact that the Level 0-1 pipeline previously replaced pixels *thought* to be well within the gap with zeroes. In a few instances where this study uncovered gaps seemingly tilted on one side by as much as a pixel, it was found that the width was changing (rather than the gap center), due in turn to changes in the slope of the gap profile edges. Scattered light as a function of the Sun's orientation with respect to the slit may have been a contributing factor.

Table 1. Measured Gap Widths.

Type	Date (yyyy.mm.dd)	Time		Gap (pixels)	<i>continued...</i>				
		VSM (hh:mm)	Reference (hh:mm:ss)		(yyyy.mm.dd)	(hh:mm)	(hh:mm:ss)	(pixels)	
6302L	2011.05.06	14:50	14:54:45	76.4	8542L	2011.05.19	15:15	15:36:45	83.7
6302L	2011.04.27	14:34	14:39:00	76.2	8542L	2010.12.06	15:53	16:15:00	77.2
6302L	2011.04.11	15:13	15:18:00	79.1	8542L	2010.08.27	15:23	15:45:00	80.3
6302L	2011.04.05	14:42	14:47:15	73.8	8542L	2010.08.02	21:24	21:45:45	77.6
6302L	2011.04.01	14:42	14:47:15	75.0	8542L	2010.07.04	22:20	22:42:00	74.4
6302L	2011.03.28	14:50	14:55:30	76.2	1083I	2011.05.28	18:02	18:09:22	80.6
6302L	2011.03.12	16:34	16:39:00	79.6	1083I	2011.05.22	15:35	15:39:22	81.5
6302L	2011.03.02	15:47	15:53:15	77.0	1083I	2011.05.14	18:04	18:09:22	82.6
6302L	2010.12.08	15:41	15:45:45	73.9	1083I	2011.04.01	16:42	16:49:22	79.9
6302L	2010.08.09	15:57	16:02:15	78.4	1083I	2011.03.28	17:35	17:39:22	85.1
8542L	2011.11.10	18:10	18:32:15	83.3	1083I	2011.03.14	16:46	16:49:23	83.0
8542L	2011.10.18	15:28	15:50:15	79.2	1083I	2011.03.05	15:41	15:49:22	78.3
8542L	2011.10.09	16:24	16:45:45	83.5	1083I	2011.01.27	19:51	19:59:22	82.7
8542L	2011.10.03	15:25	15:47:15	80.6	1083I	2011.01.24	20:54	20:59:22	80.4
8542L	2011.06.23	15:05	15:27:00	79.7	1083I	2011.01.19	18:23	18:29:22	82.9

3 Absolute Spatial Extent Measurements of the Gap

Due to the finite sharpness of the spatial beamsplitter tip, the transition between fully-illuminated and unilluminated portions of the cameras spans several pixels. Additionally, the presence of scattered light degrades, to varying degrees, the slope of the gap profile edges. In order to distinguish columns containing diminished, but valid, data from those inside the gap that are masked by stray light, the true spatial extent of the gap was carefully and independently measured for ten 6302Å, 8542Å, and 10830Å full-disk observations (see Table 1). This was done by comparing Level-1 data containing the gap to nearly simultaneous observations of the Sun taken at similar wavelengths with other instruments employing a single camera. HMI 6173Å magnetograms (`hmi.M_45s.yyyymmdd_hhmmss_TAI.2.magnetogram.fits`) and ISOON 10830Å (line center minus wing) intensity images (`yyymddhhmmssyc.fits`) were used as references for the 6302L/8542L (the wing of the 8542Å line is essentially photospheric) magnetograms and 1083I equivalent width images, respectively. Both the HMI and ISOON pixel scales (0.5" and 1.1") are comparable to the VSM's 1" pixels, and all of the reference images were made within three minutes of the midpoint of the corresponding VSM observations.

For each pair of VSM and reference images, the latter was rotated, resampled, and shifted in order to achieve rough alignment. Then, vertical 200×150 pixel regions to the left and right of the disk center (and the gap) were used to cross-correlate the two images. The difference in the cross-correlation peak coordinates between the left and right regions is equal to the number of additional columns present in the VSM image due to the gap. The gap widths (provided in Table 1 and displayed in Figure 3) were also measured using two other methods: centroiding of discrete features and visual inspection. In addition to being much more time-intensive, these approaches utilize less spatial information and are more sensitive to systematic biases such as geometry distortions across the disk. However, they provided a useful consistency check.

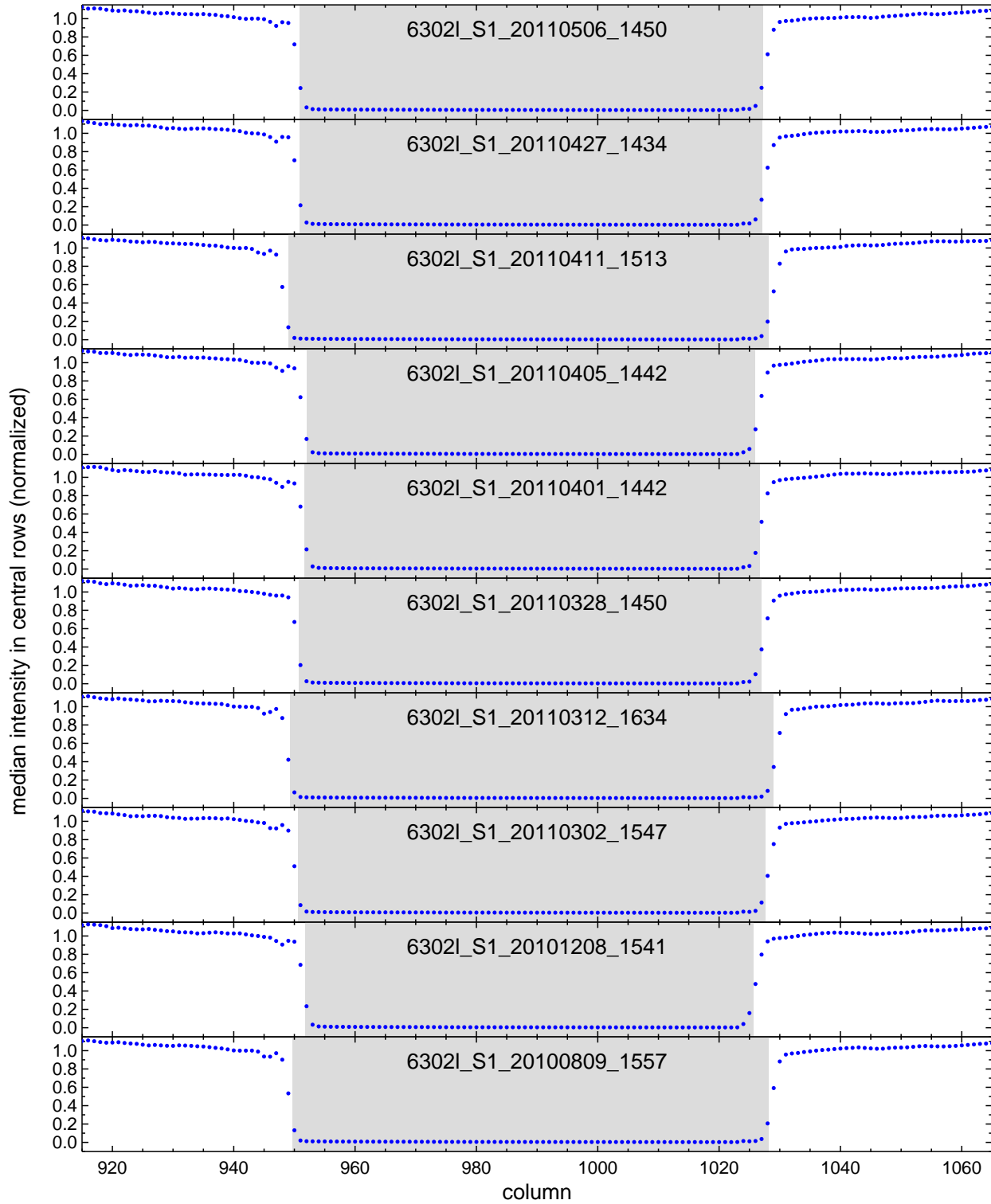


Figure 3 – Taken from the un-flat-fielded intensity images, these gap profiles are the median of the 20 most central rows normalized (separately to the left and right of column 990) by the median of the intensities within 3-13 pixels of the gap. The independently measured gap widths listed in Table 1 are indicated by the shaded regions that have been centered on each gap profile.

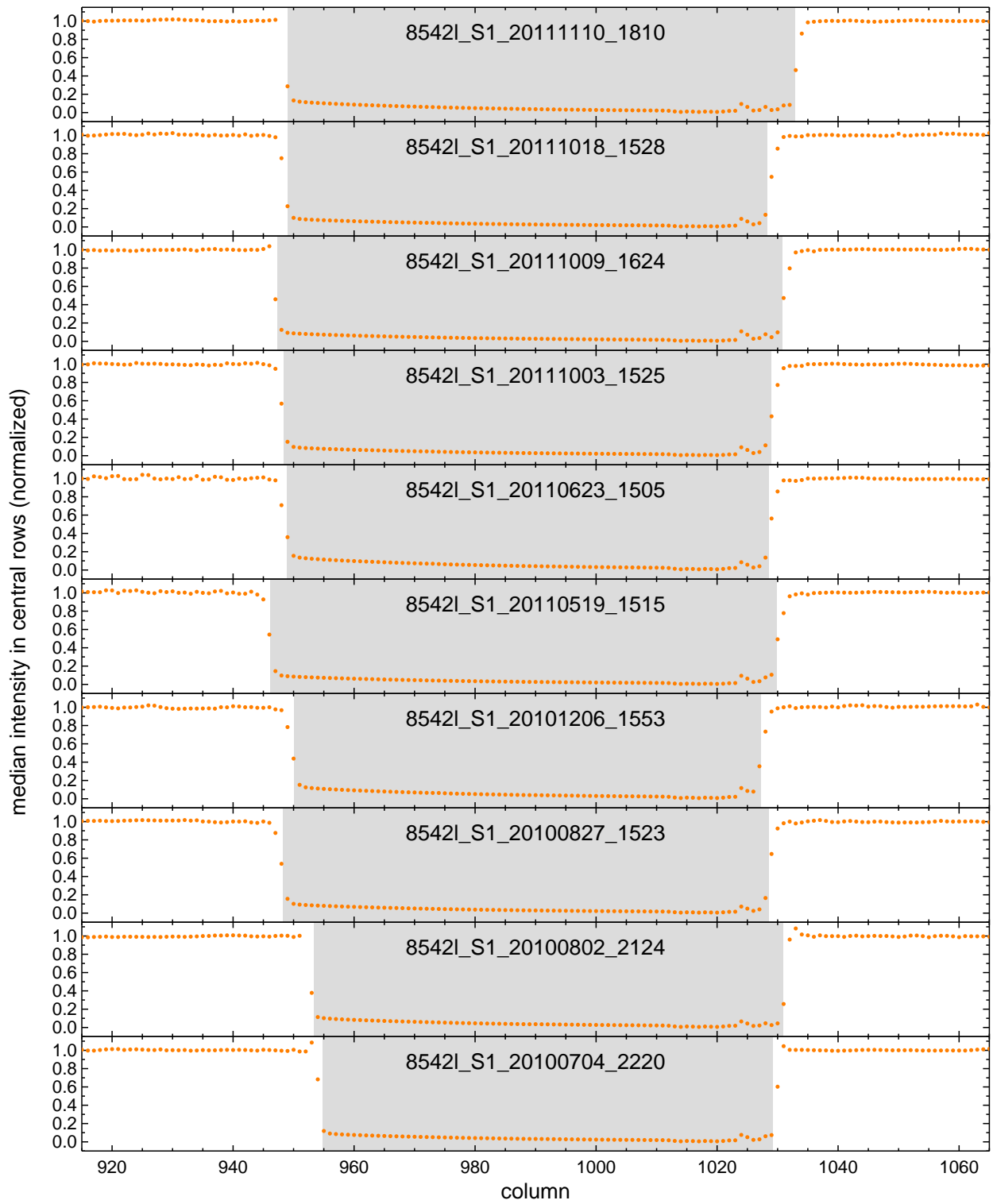


Figure 3 continued...

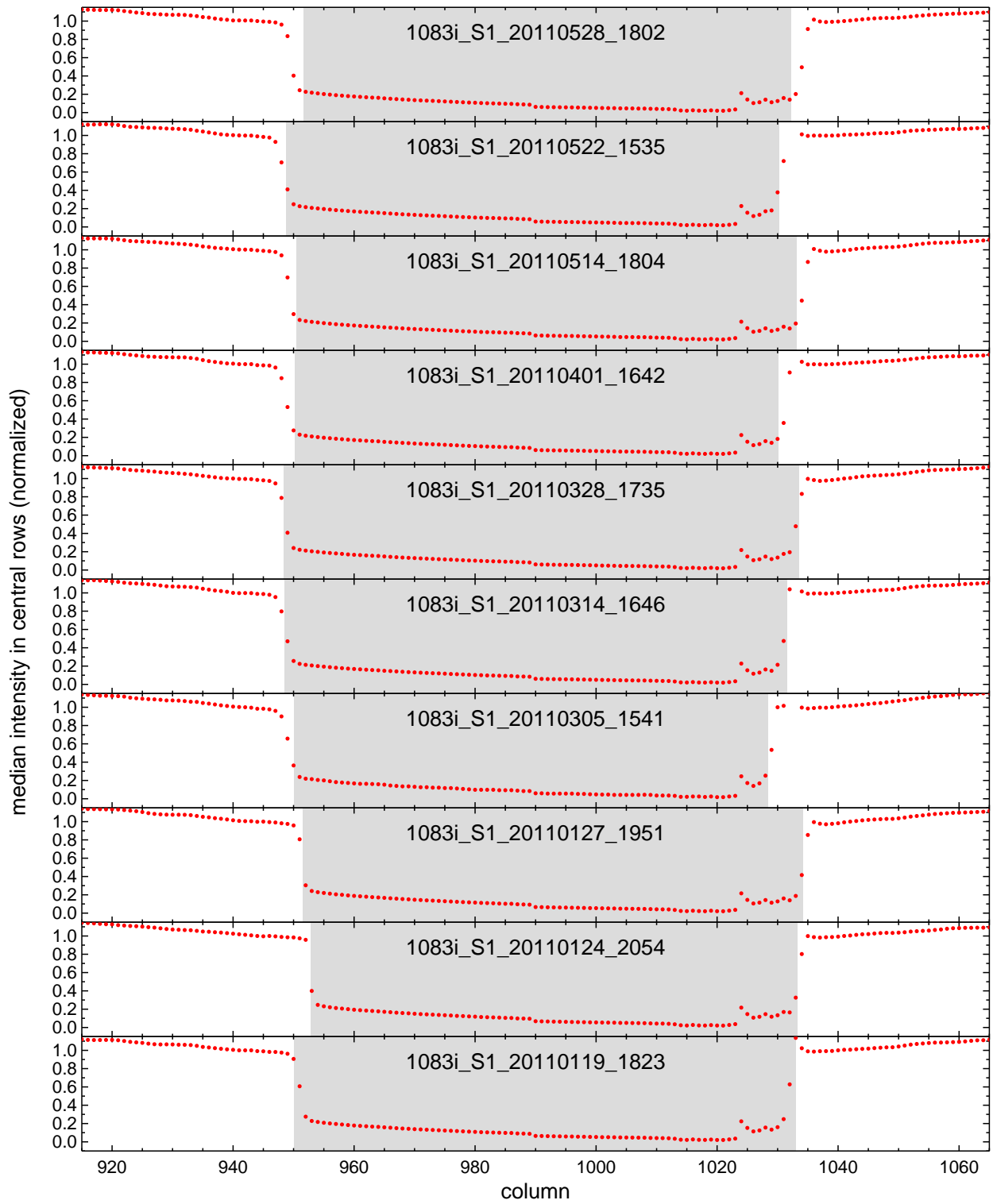


Figure 3 continued...

4 Gap Profile Intensity Thresholds

Figure 3 shows the central row gap profiles for the thirty observations with independently measured gap widths. These profiles come from un-flat-fielded intensity images produced specifically for this analysis. Flat-fielding is not valid inside the gap and results in computationally distorted profiles due to division of very small numbers by other very small numbers. Each undistorted gap profile is the median of the twenty most central rows, normalized separately to the left and the right of column 990 by the median of 10 columns just outside of the gap. The edges of the shaded regions corresponding to the gap width measurements in Table 1 similarly intersect the profiles near 50% of the fully-illuminated intensity (there is greater variance for the 1083I images due to less certain gap width measurements related to decreased contrast and worse seeing in both the infrared VSM observations and the corresponding ground-based reference images).

The actual (interpolated) intensity thresholds corresponding to the measured gap widths are plotted as diamonds in Figure 4. Similarly, values yielding widths too large and too small by one or two columns are included (the latter become indistinguishable once the flat parts of the profile are reached). There is excellent agreement between the 6302L and 8542L observations, where the mean thresholds of 30% and 36% match the measured gap widths to the nearest integer in all cases. The poorer agreement between the 1083I observations is consistent with the comparatively less certain gap width measurements and is mitigated by once again adopting the mean threshold (48%). The correlation between threshold value and wavelength is expected due to relative contributions from scattered light.

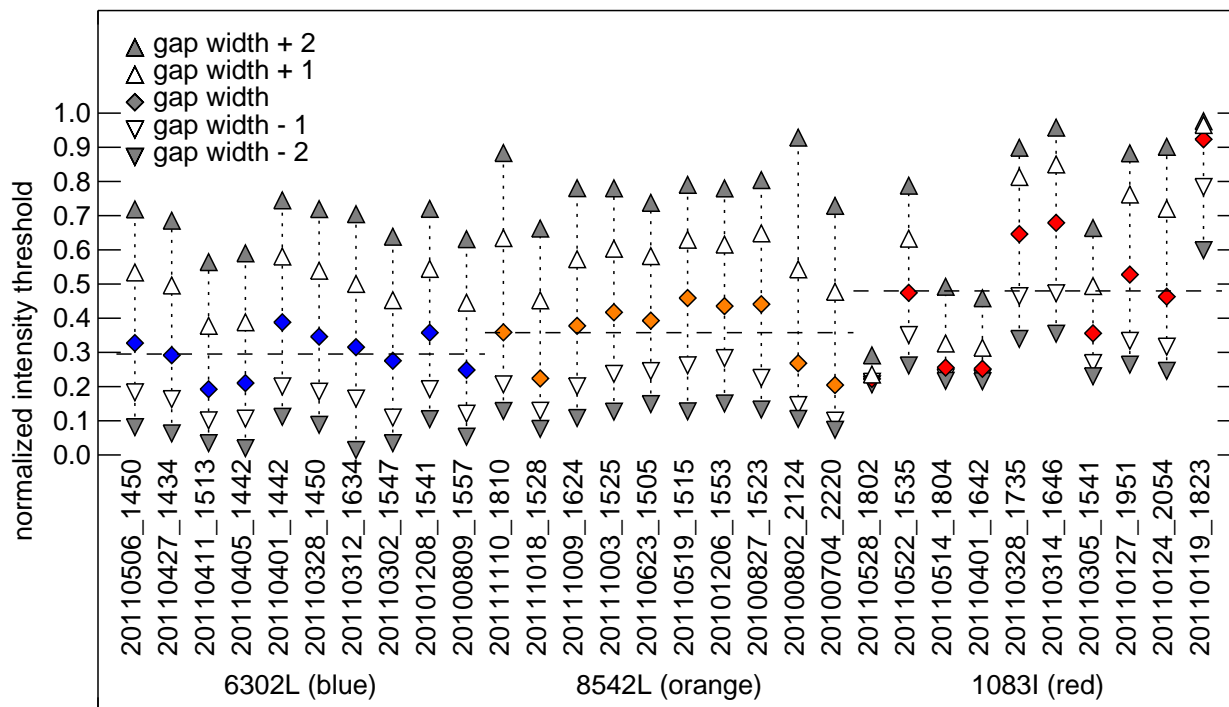


Figure 4 – Normalized intensity thresholds corresponding to the gap widths independently measured for ten 6302L (blue), 8542L (orange), and 1083I (red) observations.

5 A New Gap Removal Prescription

Beginning with the Level-0 to Level-1 pipeline versions (indicated by PROVER0) 11.1014, 12.0403, and 13.1001, respectively, for 6302L/1083I, 8542L, and 6302V data, the GAPCOL1 and GAPCOL2 keywords in the Level-1 headers correctly identify the first and last extraneous columns inside the gap. These values are determined using the following prescription, which, based on § 3 and § 4 yields gap widths that are correct to within approximately $1''$ (one column).

Take the median profile for the 20 most central rows in the un-flat-fielded intensity image, and assume a threshold X of 0.30 for 6302[L/V], 0.36 for 8542L, or 0.46 for 1083I (see § 4). Start at the index of the central column plus 20, and move towards lower column numbers. GAPCOL1 is then the first (one-indexed) column i to satisfy the condition that the intensities in columns $i-2$ and $i-1$ are greater than X times the median of the intensities in columns $i-13 : i-3$ whereas columns i and $i+1$ have intensities less than the same threshold. Symmetrically, GAPCOL2 is the first (one-indexed) column j that is greater than the central column index minus 20 where columns $j-1$ and j have intensities less than X times the median of the intensities in columns $j+3 : j+13$ while columns $j+1$ and $j+2$ are greater than the same threshold.

If the input Level-1 file predates these PROVER0 values, then GAPCOL1 and GAPCOL2 are redefined during Level-1 to Level-2 processing by applying the algorithm above to a single central row of the flat-fielded intensity image (essentially the same prescription described in Appendix A, but utilizing the newly determined relative intensity thresholds).

The Level-1 to Level-2 pipeline then simply removes the extraneous columns from all fits frames and records this fact in the header. Columns GAPCOL1-5 through GAPCOL1+4 (the five zero-indexed columns on either side of where the gap was) are re-scaled in order to account for diminished intensity near the gap. This diminution is not necessarily constant for all rows (see Figure 5) due to the changes in the gap profile wings discussed in § 2. Although scattered light (which should be subtracted rather than scaled) may be partially responsible for these changes, it is not necessarily the primary cause. Therefore, each column is simply divided by a quadratic polynomial fit to the intensity ratio of that column divided by an unaffected column (actually the median of several columns) further offset from the gap.

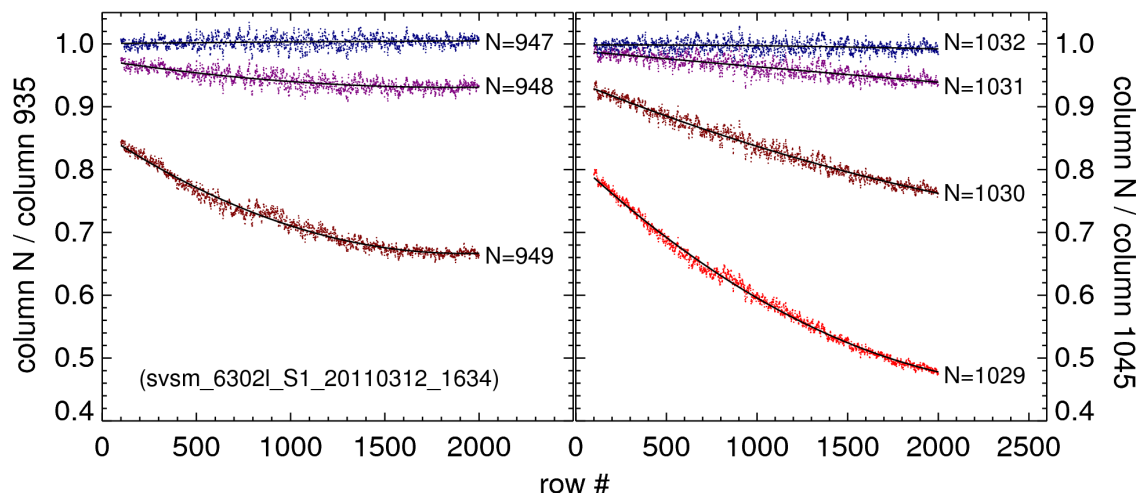


Figure 5 – Diminished relative intensity near the gap (the gap is columns 950 – 1028 in this case) is corrected for via division of the affected columns by the corresponding quadratic polynomial fits (black lines).

Appendix A Previous Gap Removal Methodology

The gap removal process described in this document went into effect in October 2011 for 6302L and 1083I, April 2012 for 8542L, and October 2013 for 6302V (due to varying, and unrelated, pipeline development considerations). For observations processed to Level-1 prior to these dates, the gap was identified and removed as described below. While not well documented, this less accurate and unnecessarily redundant methodology is likely the by-product of successive layers of modification during the early development of the data processing pipeline. The resulting gap widths and locations were generally in error by up to several pixels and by as many as tens of pixels in extreme cases. This loss of data (and the corresponding spatial information necessary for fitting and removing geometric distortions accurately) lead to the revised methodology that is the subject of this document.

First, during Level-0 to Level-1 processing (except for the earliest versions of the pipeline), the first and last pixels inside the gap were identified and written to the header (and database) as `GAPCOL1` and `GAPCOL2`, respectively, based on a single row from the corresponding flat. `GAPCOL1` was defined as the last pixel to the left of the gap center that falls below a threshold of 0.2 times the median of the pixels to the left of the gap. Likewise, `GAPCOL2` was the last pixel to the right of the gap center to fall below such a threshold; however, the scale factor used was 0.4 in this case.

Then, for 6302L and 8542L observations, `GAPCOL1` and `GAPCOL2` were used as starting values (if not available, default starting values were adopted instead) for re-determining the limits of the gap during Level-1 to Level-2 processing using the central row of the intensity image rather than the flat. The index i of the last valid pixel to the left of the gap was defined to be the instance closest to the center of the gap where pixels $i - 2$ through i all lay above 0.92 times the median of pixels `GAPCOL1 - 30` through `GAPCOL1 - 11`. Similarly, the index j of the first valid pixel to the right of the gap was taken to be the closest occurrence to gap center of pixels j through $j + 2$ being above the same threshold with respect to the median of pixels `GAPCOL2 + 11` through `GAPCOL2 + 30`.

In the case of 1083I observations, re-determining the gap limits was deemed too difficult due to “light in the gap”. It should be noted that the gap profile of 1083I intensity images is not, in fact, significantly different than the observations at other wavelengths. Although scattered light does affect the gap profile, the perceived excess light referred to above was really an algorithmic flat-fielding distortion due to, ironically, a lack of illumination inside the gap. This was not seen at other wavelengths due to masking that was not being applied to 1083I data. Rather than re-determine the gap limits, the last valid pixel to the left of the gap and the first valid pixel to the right of the gap were defined to be `GAPCOL1 - 2` and `GAPCOL2 + 2`, respectively. The subtraction/addition of a second pixel appears to be intended to compensate for a systematic error in, at least, the determination of `GAPCOL1`.

The gap was then closed by replacing those columns with indices greater than i and less than j (using the notation from above) with a single column equal to the mean of columns i and j . This, however, was not done to 6302V observations, for which the gap was already closed (by discarding columns `GAPCOL1 + 2` through `GAPCOL2 - 2`) during Level-0 to Level-1 processing for logistical reasons.